

See discussions, stats, and author profiles for this publication at: <https://www.researchgate.net/publication/231242156>

Langmuir–Blodgett Monolayer Masked Chemical Etching: An Approach to Broadband Antireflective Surfaces

ARTICLE *in* CHEMISTRY OF MATERIALS · MAY 2009

Impact Factor: 8.35 · DOI: 10.1021/cm802758e

CITATIONS

14

READS

24

6 AUTHORS, INCLUDING:



Nan Lu

Jilin University

73 PUBLICATIONS 1,406 CITATIONS

SEE PROFILE



Hongbo Xu

50 PUBLICATIONS 535 CITATIONS

SEE PROFILE



Gao Ligu

Jilin University

10 PUBLICATIONS 218 CITATIONS

SEE PROFILE



Lifeng Chi

Soochow University (PRC)

337 PUBLICATIONS 6,376 CITATIONS

SEE PROFILE

Langmuir–Blodgett Monolayer Masked Chemical Etching: An Approach to Broadband Antireflective Surfaces

Juanyuan Hao,[†] Nan Lu,^{*,†} Hongbo Xu,[†] Wentao Wang,[†] Liguao Gao,[†] and Lifeng Chi^{*,‡}

State Key Laboratory of Supramolecular Structure and Materials, Jilin University, 130012 Changchun, P. R. China, and Physikalisches Institut und Center for Nanotechnology (CeNTech), Westfälische Wilhelms-Universität, D-48149 Münster, Germany

Received October 10, 2008. Revised Manuscript Received March 9, 2009

We report a simple bottom-up approach for the fabrication of highly antireflective optical surfaces. The Langmuir–Blodgett (LB) monolayer with domain structures was used as a mask for selective etching of Si in a KOH solution. The obtained pyramidal structures can reduce the reflectivity to less than 6% at the wavelengths from 400 to 2400 nm. This technique combines the simplicity and scalability of self-assembly and cost benefits of chemical etching. These antireflective structures may have potential applications in optical devices and solar cells. Moreover, the reflectivity of polymer materials can also be reduced by transferring the pyramidal structures onto their surfaces via molding and nanoimprint lithography (NIL).

Introduction

Antireflective surfaces have recently attracted much interest because of their various applications in solar cells,^{1,2} electro-optical devices,³ and sensors.^{4,5} For the Si-based optical and optoelectronic devices, the performance is still severely limited by the high Fresnel reflection on the Si surface, which is the surface reflection of an incident light resulting from the large refractive index discontinuity at the interface of two media. Usually, multilayered thin films with intermediate or gradient refractive indices are employed to suppress the unwanted Fresnel reflection.^{6–10} However, a multilayered thin film has problems of stability induced by adhesiveness and thermal mismatch. Because the antireflection was discovered on the corneas of nocturnal moth eyes,¹¹

subwavelength structures (SWSs) have been widely used for the antireflection, in which the dimensions are smaller than the wavelength of incidence light.^{12–22} The SWSs surface is more stable and durable than a multilayered film because it is fabricated from a single material. The basic principle of this technique is to introduce a gradient refractive index by creating a structured layer between the air and the substrate material. Reflection can be substantially suppressed for a wide spectral bandwidth and over a large field of view.^{12,13} For the fabrication of antireflective structures, the dry etching method is usually applied, in which shadow masks with resolutions in subwavelength scale are required.^{14–21} The masks can be obtained by electron-beam lithography,¹⁴ laser interference lithography,^{15,16} nanoimprint lithography,^{17,18} and self-assembly.^{19–22} The practical applications, however, are still highly restricted by expensive equipment and complex

* Corresponding author. E-mail: luenan@jlu.edu.cn (N.L.); chi@uni-muenster.de (L.C.).

[†] Jilin University.

[‡] Westfälische Wilhelms-Universität.

- (1) Striemer, C. C.; Fauchet, P. M. *Appl. Phys. Lett.* **2002**, *81*, 2980.
- (2) Lee, Y. J.; Ruby, D. S.; Peters, D. W.; McKenzie, B. B.; Hsu, J. W. P. *Nano Lett.* **2008**, *8*, 1501.
- (3) Kanamori, Y.; Ishimori, M.; Hane, K. *IEEE Photon. Technol. Lett.* **2002**, *14*, 1064.
- (4) Glaser, T.; Ihring, A.; Morgenroth, W.; Seifert, N.; Schroter, S.; Baier, V. *Microsyst. Technol.* **2005**, *11*, 86.
- (5) Lee, C.; Bae, S. Y.; Mobasser, S.; Manohara, H. *Nano Lett.* **2005**, *5*, 2438.
- (6) Walheim, S.; Schaffer, E.; Mlynek, J.; Steiner, U. *Science* **1999**, *283*, 520.
- (7) Ibn-Elhaj, M.; Schadt, M. *Nature (London)* **2001**, *410*, 796.
- (8) Koo, H. Y.; Yi, D. K.; Yoo, S. J.; Kim, D. Y. *Adv. Mater.* **2004**, *16*, 274.
- (9) Wu, Z. Z.; Walish, J.; Nolte, A.; Zhai, L.; Cohen, R. E.; Rubner, M. F. *Adv. Mater.* **2006**, *18*, 2699.
- (10) Xi, J. Q.; Schubert, M. F.; Kim, J. K.; Schubert, E. F.; Chen, M. F.; Lin, S. Y.; Liu, W.; Smart, J. A. *Nat. Photonics* **2007**, *1*, 176.
- (11) Bernhard, C. G. *Endeavour* **1967**, *26*, 79.

- (12) Huang, Y. F.; Chattopadhyay, S.; Jen, Y. J.; Peng, C. Y.; Liu, T. A.; Hsu, Y. K.; Pan, C. L.; LO, H. C.; Hsu, C. H.; Chang, Y. H.; Lee, C. S.; Chen, K. H.; Chen, L. C. *Nat. Nanotechnol.* **2007**, *2*, 770.
- (13) Kanamori, Y.; Sasaki, M.; Hane, K. *Opt. Lett.* **1999**, *24*, 1422.
- (14) Kanamori, Y.; Roy, E.; Chen, Y. *Microelectron. Eng.* **2005**, *78–79*, 287.
- (15) Hadobás, K.; Kirsch, S.; Carl, A.; Acet, M.; Wassermann, E. F. *Nanotechnology* **2000**, *11*, 161.
- (16) Aydin, C.; Zaslavsky, A.; Sonek, G. J.; Goldstein, J. *Appl. Phys. Lett.* **2002**, *80*, 2242.
- (17) Yu, Z. N.; Gao, H.; Wu, W.; Ge, H. X.; Chou, S. Y. *J. Vac. Sci. Technol., B* **2003**, *21*, 2874.
- (18) Zhang, G.; Zhang, J.; Xie, G. Y.; Liu, Z. F.; Shao, H. B. *Small* **2006**, *2*, 1440.
- (19) Sai, H.; Fujii, H.; Arafune, K.; Ohshita, Y.; Yamaguchi, M.; Kanamori, Y.; Yugami, H. *Appl. Phys. Lett.* **2006**, *88*, 201116.
- (20) Sun, C. H.; Min, W. L.; Linn, N. C.; Jiang, P.; Jiang, B. *Appl. Phys. Lett.* **2007**, *91*, 231105.
- (21) Sun, C. H.; Jiang, P.; Jiang, B. *Appl. Phys. Lett.* **2008**, *92*, 061112.
- (22) Min, W. L.; Jiang, B.; Jiang, P. *Adv. Mater.* **2008**, *20*, 1002/adma.200800791.

procedures. Therefore, a simple nonlithographic technique is more desirable than dry etching because of its quite low cost. The fabrication of SWSs on Si substrate using chemical etching with spin-coated colloidal crystals as masks has been demonstrated.²³ Nevertheless, for practical applications, techniques to fabricate broadband antireflective SWSs with fewer procedures and lower cost are still strongly desired.

In this article, we report a simple method to fabricate high-density antireflective pyramidal structures on single-crystal Si substrates, which is realized by an anisotropic KOH etching of Si substrate with the mask of LB monolayer consisting of domain structures. By means of the Si pyramidal structures, the reflection of bare Si wafer is reduced to less than 6% from above 35% at the wavelengths from 400 to 2400 nm. Moreover, the pyramidal structures can be transferred to polymer materials by molding and NIL. The reflectance of polymer is reduced in the measured wavelengths.

Experimental Section

Materials. Stearic acid (STA) (chemical purity 99.7%) was obtained as a powder from Fluka. The substance was dissolved in chloroform (HPLC grade) with a concentration of 1 mg/mL. Branched poly-(ethyleneimine) (50 wt % solution in water) with an average molecular weight of 750 000 (PEI₇₅₀₀₀₀) purchased from Aldrich was dissolved in Millipore water (water resistance 18.2 M Ω cm), providing an aqueous solution with a concentration of 0.25 g/L. The substances were used without further purification. Si (100) wafers with native oxide layer were sliced into 2 \times 5 cm² pieces for the LB transfer. KOH was purchased from commercial source and was dissolved in Millipore water before use. A kit of a poly(dimethylsiloxane) (PDMS) prepolymer (Sylgard 184 silicone elastomer curing agent) was purchased from Dow Corning Corporation. Poly(methyl methacrylate) (PMMA) (ME303005) sheets were purchased from Goodfellow Corporation, USA.

LB Transfer. Si substrates (2 \times 5 cm²) were cleaned with the standard RCA method.²⁴ The substrates were stored under pure water after treatment and used within 1 h. The LB films were prepared using a commercial LB trough (NIMA 312D). The temperature of the subphase (PEI₇₅₀₀₀₀ solution 0.25 g/L) was controlled by a thermostat (25.0 \pm 0.3 $^{\circ}$ C) and the humidity of the laboratory was 20–40%. After the STA solution was spread onto the surface, the solvent was allowed to evaporate for 10 min. The resulting monolayer was then compressed to the middle position of the liquid expanded (LE) and liquid condensed (LC) coexisting region (as the arrow pointed in Figure S1 of the Supporting Information) and allowed to rest for another 15 min. The monolayer was transferred onto the Si substrate by a vertical dipping method with an upward motion at a constant dipping speed (4 mm min⁻¹).

Etching in KOH Solution. A plastic beaker with a magnetic stirrer was used as an etching bath; a hot plate with temperature control probe was used for the bath heating. Etching was carried out by immersion of the sample in the KOH solution (0.1 M) at 60 $^{\circ}$ C. The height of the produced Si arrays was controlled by etching duration. The sample was then rinsed with deionized (DI) water.

Formation of Pyramidal Structures on PMMA Substrate. The molds were prepared by casting a 10:1 (volume) PDMS/curing agent (Sylgard 184, Dow Corning) onto the etched Si substrate. After being treated under a vacuum (0.09 MPa) for 1 h to remove the

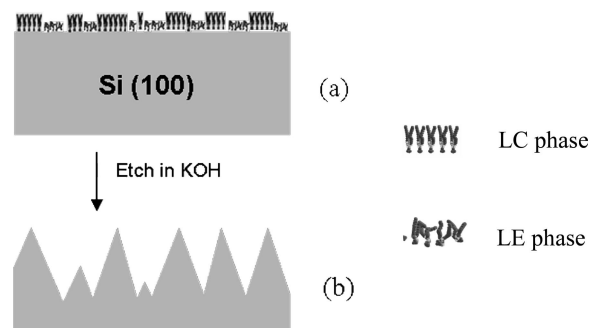


Figure 1. Schematic diagram of the fabrication process of the pyramidal arrays on a Si (100) wafer.

entrained gas and cured in a conventional drying oven at 60 $^{\circ}$ C for 6 h, the PDMS molds were peeled from the etched Si substrate. The thickness of these PDMS substrates was approximately 2 mm. Using this PDMS mold, pyramidal structures were fabricated on PMMA substrate using NIL with Obducat nanoimprinting equipment. The mold and PMMA substrate were brought into contact at 160 $^{\circ}$ C, and a pressure of 40 bar was applied for 10 min. The separation of the stamp and the substrate was made at 70 $^{\circ}$ C.

Characterization. An atomic force microscopy (AFM) image of the monolayer was acquired in ambient conditions at room temperature with a commercial instrument (Digital Instruments, Santa Barbara, CA) operating in tapping mode. Silicon cantilevers (Nanosensors, Digital Instruments) with spring constants 250–350 kHz were used. Scanning electron microscope (SEM) micrographs were taken with a JEOL JSM 6700F field emission scanning electron microscope with primary electron energy of 3 kV, and the samples were sputtered with a layer of Pt (ca. 2 nm thick) prior to imaging to improve conductivity. Spectra were collected on spectroscopy meter (Shimadzu UV3600, Shimadzu, Japan).

Results and Discussion

The fabrication process is schematically shown in Figure 1. In the previous work, the monolayer behavior of stearic acid complexed to poly-(ethyleneimine) (PEI) at the air/water interface was investigated.²⁵ With PEI dissolved in the aqueous subphase, in contrast to pure water, the form of the π/A isotherm of stearic acid was drastically changed from an incompressible monolayer to an expanded one at the air/water interface, and undergoes an additional fluid/solid phase (LE/LC) transition. Through the interaction with polymeric gegenions, domains formed in coexistence region (LE+LC). In this work, with the PEI aqueous as subphase, the STA molecules were initially transferred onto the Si substrate [n type, (100)] using the LB technique to obtain the etching mask (Figure 1a). As revealed by the AFM measurement (Figure 2), the STA monolayer is composed of LC STA domains and the surrounded LE STA molecules.^{26,27} The average size of domains is around 1 μ m. The size and space of the domains can be changed by adjusting the LB preparation parameters.²⁵ Second, the Si substrate with the STA monolayer was etched by immersing it into a 0.1 M 60 $^{\circ}$ C KOH aqueous solution (Figure 1b). As shown in Figure 3a, 500 nm high truncated Si pyramidal structures were fabricated after 7 min etching. It can be observed that

(25) Chi, L. F.; Johnston, R. R.; Ringsdorf, H. *Langmuir* **1991**, 7, 2323.

(26) Chi, L. F.; Anders, M.; Fuchs, H.; Johnston, R. R.; Ringsdorf, H. *Science* **1993**, 259, 213.

(27) Chi, L. F.; Gleiche, M.; Fuchs, H. *Langmuir* **1998**, 14, 875.

(23) Wang, S.; Yu, X. Z.; Fan, H. T. *Appl. Phys. Lett.* **2007**, 91, 061105.

(24) Brzezinski, V.; Peterson, I. R. *J. Phys. Chem.* **1995**, 99, 12545.

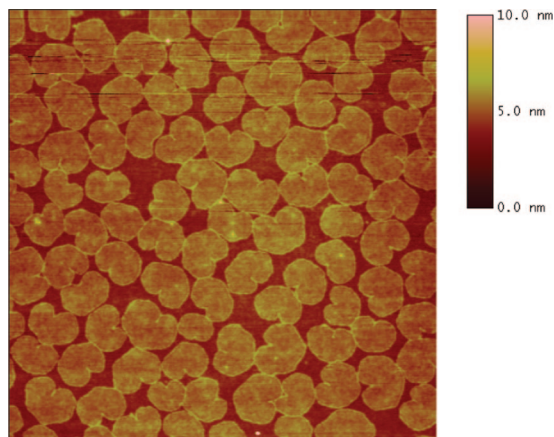


Figure 2. AFM image of STA monolayer on Si substrate. Scan size: $10 \times 10 \mu\text{m}$.

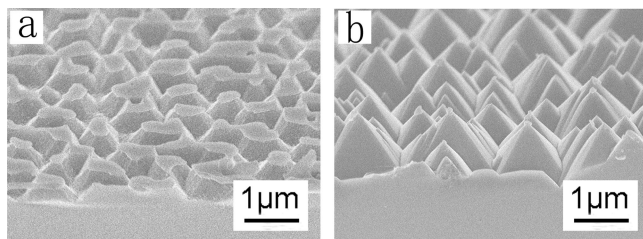


Figure 3. Cross-sectional SEM images of the Si pyramidal arrays etched for (a) 7 and (b) 10 min.

the LE covered regions were selectively etched because of their higher wettability and loosely packing.^{28–30} The etched sample presents an anisotropic angle of 54.7° , which is the typical alkaline etching angle of the Si [100] surface. The density of the pyramidal arrays is well consistent with that of the STA domains (see the Supporting Information, Figure S2). The average height of the Si pyramids can be controlled by adjusting the etching duration. Further extending the etching duration to 10 min, the average height of Si pyramids increased to 700 nm, and the pyramids changed from truncated to tapered shape (Figure 3b).

The optical microscopy measurement demonstrates the different antireflective behaviors of the Si pyramidal arrays and the unetched Si surface (Figure 4a). The unetched top part is mirrorlike, whereas the bottom part with the Si pyramidal arrays (etched for 10 min) displays much lower reflection. The reflectivity is further measured using a spectrometer at normal incidence over a wavelength ranging from 400 to 2400 nm. Figure 4b shows the measured reflection for a bare Si wafer and Si pyramidal arrays etched for 7 and 10 min, respectively. The Si wafer exhibits a high reflection for all measured wavelengths (dotted line), consistent with previous measurement.^{31,32} The 7 min etched sample (solid line) presents lower reflection and wavelength-

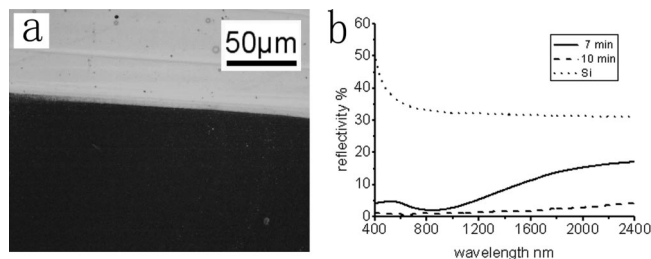


Figure 4. (a) Optical microscopy image of Si pyramidal arrays etched for 10 min (bottom part) and bare Si wafer (top part), the former demonstrates antireflective behavior. (b) Specular optical reflection at normal incidence for a bare Si wafer (dotted line) and Si pyramidal arrays etched for 7 min (solid line), and 10 min (dashed line).

dependent reflectivity: it is below 4% at the wavelengths from 600 to 1100 nm, and less than 17% at wavelengths from 1100 to 2400 nm. Much lower reflectivity is achieved on the 10 min etched Si sample (dashed line), which is less than 2% for wavelengths from 400 to 1200 nm, and remains below 6% at wavelengths from 1200 to 2400 nm. The result suggests that lower reflectivity can be obtained by increasing the aspect ratios of the Si arrays and making the Si arrays tapered. Most importantly, the resulting antireflectivity is broadband, ranging from visible and near-infrared wavelengths. Control experiments were done by etching a bare Si wafer. Because of contact angle, gas bubble detachment, and surface roughness, pyramidal structures are also formed.³³ Under the same etching conditions, however, the density of the pyramids is much lower, thus resulting in a slight decrease of the reflectivity at the wavelengths from 400 to 2400 nm (see the Supporting Information, Figure S3).

The Fresnel reflection can be reduced by inserting a layer with intermediate index⁶ or multilayer with stepped refractive index.³⁴ According to effective medium theory, the array of conical protuberances having sinusoidal profiles can result in a gradient refractive index between the air and the substrate, dramatically reducing the reflection at the surfaces. For ideal array with near zero reflectivity, the effective refraction index n_{eff} value should gradually increase from 1 to n_{Si} from the boundary of air/array to the boundary of array/Si. This requires the perfectly tapered shapes of arrays and grooves. Appropriate heights of SWSs are also needed for minimizing reflection losses. The strong suppression of reflection happens when the ratio of the thickness of array layer to wavelength is greater than 0.4. By further increasing the array height, the reflectivity will slightly fluctuate and approach zero.¹⁵

As revealed in Figure 3a, the 7 min etched pyramids have flat tops, which induce an abrupt increase of n_{eff} at the interface of air/array leading to a higher residual reflection (4–17%). When the Si pyramids were changed from truncated (Figure 3a) to tapered (Figure 3b) by extending the etching duration to 10 min, the n_{eff} is approaching to 1 at the interface of air/array. As presented in Figure S4 of the Supporting Information, there is no flat area at the bottom of neighbored tapered pyramids, which results in the n_{eff} at

(28) Lenhart, S.; Zhang, L.; Mueller, J.; Wiesmann, H. P.; Erker, G.; Fuchs, H.; Chi, L. F. *Adv. Mater.* **2004**, *16*, 619.

(29) Chen, X. D.; Lenhart, S.; Hertz, M.; Lu, N.; Fuchs, H.; Chi, L. F. *Acc. Chem. Res.* **2007**, *40*, 393.

(30) Hao, J. Y.; Lu, N.; Wu, Q.; Hu, W.; Chen, X. D.; Zhang, H. Y.; Wu, Y.; Wang, Y.; Chi, L. F. *Langmuir* **2008**, *24*, 5315.

(31) Yu, Z. N.; Gao, H.; Wu, W.; Ge, H. X.; Chou, S. Y. *J. Vac. Sci. Technol. B* **2003**, *21*, 2874.

(32) Kanamori, Y.; Hane, K.; Sai, H.; Yugami, H. *Appl. Phys. Lett.* **2001**, *78*, 142.

(33) Baum, T.; Satherley, J.; Schiffrin, D. J. *Langmuir* **1998**, *14*, 2925.

(34) Rajteri, M.; Rastello, M. L.; Monticone, E. *Nucl. Instrum. Methods Phys. Res., Sect. A* **2000**, *444*, 461.

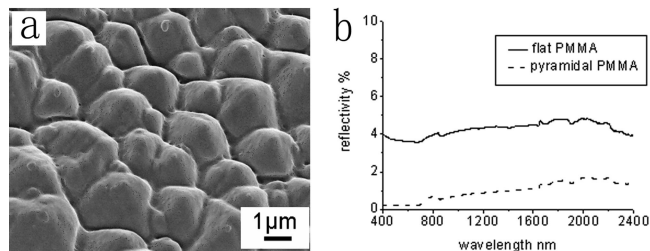


Figure 5. (a) Top-view SEM image of the imprinted PMMA film. (b) Specular optical reflection at normal incident angle for the imprinted PMMA film with the pyramidal structures (dashed line) and a flat PMMA film (solid line).

the interface of array/Si approaching to n_{Si} . Thus, the 10 min etched sample exhibits much lower residual reflection (2–6%). In addition, the height of the pyramids is determined by the distance between the two adjacent domains due to the characteristic 54.7° sidewalls. At the wavelengths from 1750 to 2400 nm, the ratio of Si array height to the wavelength is smaller than 0.4, which should be the main reason for the increased residual reflection.

These antireflective structures on Si can be easily replicated onto some polymer materials, e.g., PMMA sheet. The replication procedure is schematically shown in Figure S5 (see Supporting Information). This mainly involves a two-step replica molding: first, a negative PDMS mold is prepared by directly molding the antireflective Si structures; subsequently, the PDMS mold is used as a stamp for NIL to obtain the replica of the pyramidal structures on polymer substrate. The SEM image of the imprinted pyramidal structures on PMMA substrate is shown in Figure 5a. Figure 5b shows the comparison of reflectivity for imprinted PMMA film with

a flat PMMA film. The pyramidal structures on PMMA substrate reduce the reflectivity from 4.3 to 0.9% at wavelength of 1200 nm.

Conclusions

In conclusion, antireflective Si surfaces over a large area were fabricated by LB monolayer masked chemical etching. By means of the LB etched pyramidal structures, the reflectance of Si is uniformly reduced to below 6% in the wavelengths between 400 and 2400 nm. The height of the Si pyramids can be controlled by adjusting KOH etching duration. Furthermore, the Si pyramidal arrays can be replicated on the polymer substrates by imprinting with a stamp molded from the Si pyramidal arrays, which leads to a suppressed reflectance of e.g. PMMA sheet to below 1.6% in the wavelengths between 400 and 2400 nm. It should be possible to further lower the reflection by reducing the size of LB domain. This method may provide a new route for the fabrication of antireflective Si, which can be used for the crystalline Si-based optical devices and solar cells. Combined with NIL, it provides a general strategy of fabrication polymer materials with antireflective structures.

Acknowledgment. Financial support was given by the National Natural Science Foundation of China (20773052, 20373019, and 50520130316), the NCET Program, the National Basic Research Program (2007CB808003, 2009CB939701), and 111 Project (B06009).

Supporting Information Available: Additional figures (PDF). This material is available free of charge via the Internet at <http://pubs.acs.org>.

CM802758E